HHS Public Access

Author manuscript

Int J Radiat Oncol Biol Phys. Author manuscript; available in PMC 2023 July 01.

Published in final edited form as:

Int J Radiat Oncol Biol Phys. 2022 July 01; 113(3): 661–674. doi:10.1016/j.ijrobp.2022.02.019.

Total-Body Irradiation Is Associated With Increased Incidence of Mesenchymal Neoplasia in a Radiation Late Effects Cohort of Rhesus Macaques (*Macaca mulatta*)

W. Shane Sills, DVM, DACVP[*], **Janet A. Tooze, PhD**[†], **John D. Olson, MS**[*], **David L. Caudell, DVM, PhD**[*], **Greg O. Dugan, DVM**[*], **Brendan J. Johnson, DVM**[*], **Nancy D. Kock, DVM, PhD, DACVP**[*], **Rachel N. Andrews, DVM, PhD, DACVP**[*,‡], **George W. Schaaf, DVM**[*], **Richard A. Lang, DVM**[*], **J. Mark Cline, DVM, PhD, DACVP**[*,‡]

[*]Department of Pathology, Section on Comparative Medicine, Wake Forest School of Medicine, Winston-Salem, North Carolina

[†]Department of Biostatistics and Data Sciences, Wake Forest School of Medicine, Winston-Salem, North Carolina

[‡]Department of Radiation Oncology, Wake Forest School of Medicine, Winston-Salem, North Carolina

Abstract

Purpose: Cancer is a severe delayed effect of acute radiation exposure. Total-body irradiation has been associated with an increased risk of solid cancer and leukemia in Japanese atomic bomb survivors, and secondary malignancies, such as sarcoma, are a serious consequence of cancer radiation therapy. The radiation late effects cohort (RLEC) of rhesus macaques (*Macaca mulatta*) is a unique resource of more than 200 animals for studying the long-term consequences of total-body irradiation in an animal model that closely resembles humans at the genetic and physiologic levels.

Methods and Materials: Using clinical records, clinical imaging, histopathology, and immunohistochemistry, this retrospective study characterized the incidence of neoplasia in the RLEC.

Results: Since 2007, 61 neoplasms in 44 of 239 irradiated animals were documented (18.4% of the irradiated population). Only 1 neoplasm was diagnosed among the 51 nonirradiated controls of the RLEC (2.0%). The most common malignancies in the RLEC were sarcomas (38.3% of diagnoses), which are rare neoplasms in nonirradiated macaques. The most common sarcomas included malignant nerve sheath tumors and malignant glomus tumors. Carcinomas were less common (19.7% of diagnoses), and consisted primarily of renal cell and hepatocellular carcinomas. Neoplasia occurred in most major body systems, with the skin and subcutis being the

Corresponding author: J. Mark Cline, DVM, PhD, DACVP; jmcline@wakehealth.edu.

Disclosures: The authors have no disclosures.

Data sharing statement: Research data are stored in an institutional repository and will be shared upon request to the corresponding author.

most common site (40%). RNA analysis showed similarities in transcriptional profiles between RLEC and human malignant nerve sheath tumors.

Conclusions: This study indicates that total-body irradiation is associated with an increased incidence of neoplasia years following irradiation, at more than double the incidence described in aging, nonirradiated animals, and promotes tumor histotypes that are rarely observed in nonirradiated, aging rhesus macaques.

Introduction

Survivors of acute total-body irradiation (TBI) are faced with chronic health issues, including increased risks of leukemia and solid cancers. In Japanese survivors of the atomic bomb explosions, leukemia was the earliest cancer to arise, occurring after only 1 to 2 years, with peak excess cases at approximately 10 years postexposure.[1] The excess relative risk of solid cancers incidence in the Life Span Study, a cohort study following 94,000 atomic bomb survivors as well as their children since 1950, ranges from 0.47 to 0.5 per Gy,[1–3] with the highest risk associated with bladder cancers (nearly 150%).[1,2,4] Excess relative risk of all solid cancers began to increase after 0.1 to 0.2 Gy, and increased linearly in a dose-dependent manner.[1,2,4] Localized radiation, as in radiation therapy for solid cancers, is also associated with increased risk of second malignancies in the irradiated area.[5,6] Among radiation-induced neoplasms, soft tissue and bone sarcomas are rare but serious second malignancies, as these are locally aggressive, typically refractory to treatment, and associated with a poor prognosis.[5,6] Radiation-induced soft tissue sarcomas have a standardized incidence ratio of 54 in children receiving radiation therapy compared with the general population.[7] Schneider et al[8] combined the linear-no-threshold model of the Japanese Life Span Study with cancer risk data in a cohort of patients receiving radiation therapy for Hodgkin lymphoma to model cancer risk at the low- and high-dose ranges. For bone and soft tissue sarcomas, it was shown that the excess absolute risk was minimal at point doses up to 1.0 Gy, but increased rapidly with increasing dose, plateauing at 30 Gy with an excess absolute risk of approximately 2.2 to 2.4 per 10,000 persons per year.[8] These studies highlight the significance of cancer as a consequence of total-body and local irradiation. A suitable animal model would provide a valuable resource in understanding the biology of radiation-induced tumors.

Nonhuman primates (NHPs) are a useful species for modeling human disease due to their genetic, physiologic, reproductive, immunologic, and metabolic similarities to humans.[9–12] NHPs are similar to humans in the histologic and genetic features of spontaneous, infection-induced, and carcinogen-induced neoplasia.[12] As early as 1958, sarcomas were noted in rhesus macaques as a consequence of focal head irradiation with Co60 γ-rays and thermal neutrons.[13] In the early 1960s, a cohort comprising 29 irradiated and 21 nonirradiated rhesus macaques in the Netherlands was used to study acute effects of radiation and bone marrow transplantation,[14] with animals receiving either 2.3 to 4.4 Gy TBI of fission neutrons or 4.0 to 8.6 Gy TBI of x-ray. Once these studies were completed, the surviving monkeys were followed over the course of their lifetime. Irradiated animals had an 8X increase in relative risk of malignancy and a higher incidence of sarcomas relative to the control animals.[14] In 1991, Wood[15] also reported a dose-dependent increase in cancer risk and

mortality in 358 macaques exposed to protons mimicking energies of the Van Allen belt and solar proton events, monitored over 24 years. In contrast, reports of spontaneous cancer incidence in populations of rhesus macaques (*Macaca mulatta*) describe that, similar to humans, epithelial cancers are the most common solid neoplasms in aging monkeys, with mesenchymal neoplasms representing only a small portion.[16,17] Simmons and Mattison[16] described cancer incidence in two large populations of captive rhesus macaques. Out of 1100 animals, a total of 260 cancers were diagnosed in 217 animals. Intestinal carcinoma accounted for 48% of the diagnoses. These studies suggest that TBI promotes cancer in NHPs and can influence the type of cancers they develop. However, previous studies using rhesus macaques to study long-term effects and carcinogenesis from total body photon (γ- or x-ray) irradiation have been limited by number of subjects.[15] A larger cohort exposed to photon radiation is needed to build upon these initial findings.

Wake Forest School of Medicine (WFSM) is home to the radiation late effects cohort (RLEC), a one-of-a-kind, National Institute of Allergy and Infectious Diseases-supported resource of rhesus macaques acquired from various TBI studies.[18,19] This cohort was established in 2007 and includes survivors of single-dose, x-ray, and γ-ray TBI, as well as nonirradiated control animals. The RLEC has already been used to elucidate long-term effects of radiation, including type 2 diabetes,[20,21] deficiencies in cognitive flexibility,[22] cerebrovascular injury,[23,24] lung injury,[25] increased myocardial fibrosis and systemic inflammation,[26] and long-term immune impairment.[27] In this study, we describe the RLEC as an NHP model of TBI-induced cancer.

Methods and Materials

Animal population

The RLEC consists of animals irradiated at WFSM (Winston-Salem, NC); the University of Maryland (Baltimore, MD); the University of Illinois Chicago (Chicago, IL); the Armed Forces Radiobiology Research Institute (Bethesda, MD); Lovelace Respiratory Research Institute (Albuquerque, NM); and Charles River Laboratories (Laval, Quebec, Canada). This report includes 290 NHP, of which 239 (168 male, 71 female) were exposed to a single dose of TBI, with the remaining 51 (47 male, 4 female) serving as nonirradiated controls. Irradiated animals received 1.14 to 8.5 Gy total body radiation under Institutional Animal Care and Use Committee oversight at their prior institution using 1 of 2 strategies: (1) linear accelerator-derived photons at a nominal mean energy of 2 MeV, delivered at 80 cGy/minute as a split dose given half anterior-posterior and half posterior-anterior; or (2) cobalt 60-derived γ irradiation delivered simultaneously, bilaterally at 60 cGy/min. Note that these are potentially lethal doses: the lethality dose (LD) 10/30 for rhesus macaques is ~5.5 Gy, the LD 50/30 is ~6.7 Gy, and the LD 90/30 is 8 Gy.[28] Surviving animals were subsequently transferred to WFSM for long-term monitoring postradiation. Irradiation methods, supportive care strategies, and acute effects for many animals donated to this cohort have been recently reported.[18,28,29] Lethality dose groups were defined as control (0 Gy), <LD10 (>0–5.49 Gy), LD10–50 (5.5–6.74 Gy), LD50–90 (6.75–8.0 Gy), and LD90+ (>8.0 Gy), according to the LD30 of acute radiation hematopoietic syndrome in rhesus monkeys.[28] Lethality group numbers are provided in Table 1. Irradiated animals were

exposed between 2.3 to 15.5 years of age, with a median of 4.4 years (95% confidence interval, 4.2–4.6 years) and a mean of 4.8 ± 1.9 years. After arrival, animals were quarantined for 60 days, and screened for tuberculosis by intradermal tuberculin testing.

All experimental procedures at WFSM were conducted in compliance with Institutional Animal Care and Use Committee requirements. WFSM is accredited by the Association for the Assessment and Accreditation of Laboratory Animal Care International. Animals were monitored twice daily by trained technical staff for health and welfare. Monkeys were fed a diet of commercial chow (Purina LabDiet Monkey Diet 5038, Richmond, IN) prior to arrival at WFSM, after which all animals were transitioned to a Western Diet (Typical American Diet; Purina LabDiet 5L0P). Water was provided ad libitum. Housing was indoor-outdoor in social groups when possible. Animals were provided a rotating system of environmental enrichment, including toys, puzzles, climbing structures, hiding environments, and fruits/vegetables. Behavioral well-being was monitored and recommendations made by an independent behavioral management team. All animals were trained to cooperate in handling procedures to minimize stress. Animals exhibiting signs of illness were evaluated by the clinical veterinary team, independent of the research team.

Clinical assessment

Animals were assessed by daily observation, annual physical exams under chemical sedation, annual, full-body, noncontrast computed tomography scans, and triennial cranial magnetic resonance imaging. All imaging studies were conducted under general anesthesia. Tumors discovered by radiologic imaging or visual examination were monitored for growth and effect on quality of life. Biopsy procedures were conducted under either ketamine sedation (10–15 mg/kg) with lidocaine (2 mg/kg) for local anesthesia or under general anesthesia using ketamine sedation followed by isoflurane inhalation. Postoperative analgesic treatment consisting of buprenorphine (0.01–0.03 mg/kg/day) and meloxicam (0.2 mg/kg/day) or ketoprofen (5 mg/kg/day) was used for all animals. Animals with severe morbidity or pain unresponsive to analgesia were humanely euthanized due to quality of life considerations and subsequently necropsied. Euthanasia was in accordance with the American Veterinary Medical Association's Guidelines on Euthanasia.[30]

Pathology and immunohistochemistry

Pathology assessments were conducted under the supervision of board-certified veterinary pathologists. Biopsies were fixed in 4% paraformaldehyde for 24 hours, followed by 70% ethanol before embedding in paraffin and staining with hematoxylin and eosin.

For euthanized animals, tissue samples from all organ systems were collected after confirmation of death and fixed in 4% paraformaldehyde for 24 hours, followed by 70% ethanol before embedding in paraffin and staining with hematoxylin and eosin. For biopsy and necropsy samples, parallel frozen samples were collected and stored at −80C.

Tumor phenotype was determined by histopathologic assessment by a board-certified pathologist, augmented by immunohistochemical (IHC) techniques as needed. The following markers were used as needed: myeloperoxidase (catalog NCL-L-MYELO, clone 59A5; Leica Biosystems, Buffalo Grove, IL) for suspected myeloid neoplasia; CD3 (catalog

A0452, polyclonal rabbit; Dako/Agilent, Santa Clara, CA) for suspected lymphomas; vimentin (catalog ab8069, clone V9; Abcam, Cambridge, UK) for sarcomas; pancytokeratin (catalog M3515, clone AE1/AE3; Dako/Agilent) for carcinomas; S100 (catalog MA5–12969, clone 4C4–9; Thermo Scientific, Waltham, MA) for nerve sheath tumors; α-smooth muscle actin (α-SMA; catalog ab5694, rabbit polyclonal; Abcam) for suspected glomus tumors; CD31 (catalog MA5–13188, clone JC/70A; Thermo Scientific) for suspected angiosarcomas; collagen IV (catalog ab6586, rabbit polyclonal; Abcam) for suspected fibrosarcomas and glomus tumors; and tumor suppressor p53 (catalog sc-126, clone DO-1; Santa-Cruz Biotechnology, Dallas, TX). IHC was conducted as previously described.[23] Briefly, slides were loaded onto a Leica Bond RX automatic stainer (Leica Biosystems) after air-drying overnight. After dewaxing and rinsing, antigen retrieval was conducted by heat-induction in a 99°C bath for 20 minutes. The antigen retrieval bath varied depending on the antibody and consisted of either citrate buffer (pH 6.0) or ethylenediaminetetraacetic acid buffer (pH 8.0). A 10-minute incubation with immunohistochemical/*in situ* hybridization Super Blocking Novocastra solution (Leica Biosystems) was used for blocking endogenous peroxidase activity. All slides were incubated with the primary antibody for 15 min and then rinsed. Secondary antibody and chromogen application were as according to manufacturer's specifications (Bond Polymer Refine Red Detection Kit; Leica Biosystems). Slides were then removed from the instrument, dehydrated, cleared with xylene, and coverslipped.

RNA sequencing

RNA was isolated from snap-frozen tissue samples of 5 malignant nerve sheath tumors (MNSTs) (4 cutaneous, 1 renal) that were initially stored at −80°C. After rotary homogenization of flash-frozen tissue, a commercial kit (Zymo Research, Irvine, CA) was used to isolate RNA. Isolated RNA was frozen and stored at −80°C until sequenced. Total RNA was used to prepare cDNA libraries using the Illumina TruSeq Stranded Total RNA with Ribo-Zero Gold Preparation kit (Illumina, Inc). Total RNA was rRNA depleted followed by enzymatic fragmentation, reverse-transcription, and double-stranded cDNA purification using AMPure XP magnetic beads. The cDNA was end repaired, 3′ adenylated, with Illumina sequencing adaptors ligated onto the fragment ends, and the stranded libraries were pre-amplified with PCR. The library size distribution was validated and quality inspected using an Agilent Technologies 4200 TapeStation. RNA integrity numbers varied from 4.1 to 4.7. The quantity of each cDNA library was measured using the Qubit 3.0 (Thermo Fisher). The libraries were pooled and sequenced on the Illumina NovaSeq 6000.

Rhesus MNST gene expression patterns were compared to RNAseq data from the Cancer Genome Atlas (TCGA) study of sarcomas (TCGA-SARC),[31] consisting of 9 cases of MNST, from the National Cancer Institute's Genomic Data Commons (https://portal.gdc.cancer.gov/projects/TCGASARC).

RNA data analysis

Alignment of reads was performed using the Spliced Transcripts Alignment to a Reference (STAR) sequence aligner,[32] and gene expressions in counts were extracted using featureCounts.[33] Differential gene expression analysis was conducted on raw counts from 5 rhesus monkey MNSTs in the RLEC and 9 human MNSTs downloaded from the TCGA-SARC

study[31] using the R package DESeq2. Prior to analysis, rhesus and human RNA counts were merged along shared gene symbols using R software, creating a file containing counts for 12,826 genes across all 14 samples. Raw counts were normalized to housekeeping genes, including *TBP*, *TFRC*, *HPRT1*, *RPL32*, *GAPDH*, and *ACTB*, based on in vitro findings of Gu in malignant Schwann cells,[34] using the R package RUVSeq.[35] This process generated multiple unwanted variance variables, which were then included as covariates in the design of the DESeq2 data set. This allowed us to control for between-samples variation, in addition to the library-size normalization method incorporated in the DESeq2 package. Differentially expressed genes were defined as genes with an adjusted P value <.05. Gene ontology enrichment analysis was conducted on genes up-regulated in rhesus MNSTs using the online Gene Ontology Resource (http://geneontology.org/), powered by PANTHER.[36]

Statistical analysis

Descriptive statistics were used to summarize the characteristics of the cohort by lethality dose group. Tumor incidence, overall and by type, in irradiated animals were compared to controls using log-rank tests (unadjusted) and Cox regression for overall incidence (adjusted for sex) with a time axis that began at the age at arrival in the cohort to either diagnosis of the first cancer or the current age or age at death if no cancer was observed. Using age as the time axis allows for adjustment for cancer incidence risk by age that may differ between groups. The log-rank tests were adjusted for this left truncation (age at entry) using the SAS macro %lt_logranktest in SAS (version 9.4; SAS Institute, Cary, NC). For irradiated animals, tumor incidence was evaluated using both age as the time axis with time at irradiation as the entry time and time since irradiation using log-rank tests (adjusted for left truncation in the age analyses) and Cox regression (adjusted for sex and additionally for age at irradiation for the time since irradiation analyses). Distribution of tumor types for the first tumor were compared using Fisher's exact test among irradiated animals with cancer. Developing more than 1 tumor was compared by lethality dose group using Fisher's exact tests among irradiated animals with cancer. Kaplan-Meier plots were generated with Prism 8 software (version 8.4.3; GraphPad, San Diego, CA). A 2-sided $\alpha = 0.05$ was used for statistical significance.

The systemic transcriptional profiles of human and rhesus MNSTs were analyzed using principal component analysis (PCA). A matrix of log2-transformed gene expression counts was generated using variance stability transformation in DESeq2. The 1200 most variably expressed genes, ranked by standard deviation among samples, were used to conduct PCA in ClustVis software.[37] ClustVis was then used to generate a PCA dot plot.

Eleven genes involved in recurrently altered pathways in MNSTs were selected from the log2-transformed count matrix. The selected genes were *SUZ12*, *EED*, *NF1*, *TP53*, *EZH1*, *EZH2*, *ATRX*, *RB1*, *YAP1*, *AKT1*, and *mTOR*. Multiple t tests with adjustment for multiple testing were conducted on these genes, comparing means of human MNSTs to rhesus MNSTs. This analysis was conducted using Prism 8 software, and an adjusted P value of .05 was considered significant.

Results

TBI is associated with an increased incidence of neoplasia

Table 1 provides a summary of the RLEC population, grouped by radiation lethality dose group. The mean age at observation (current age as of September 30, 2021, or age at death) of the irradiated group was 9.8 ± 3.6 years, while the mean age of the nonirradiated controls was 14.4 ± 4.7 years. Irradiated animals were exposed between 2.3 to 15.5 years of age, with a median of 4.4 years. For the total RLEC, 61 neoplasms (benign or malignant) were diagnosed in 44/239 (18.4%) of the irradiated NHP group between January 2007 and September 2021 (Fig. 1). Additionally, a hepatocellular carcinoma was diagnosed in 1 male from the nonirradiated control group of 51 animals (2.0%) in that time frame. Histologic diagnoses were made by surgical biopsy in 14/61 tumors (23%), and the remaining tumors were histologically diagnosed at necropsy. Among the 44 irradiated animals with neoplasms, initial neoplasms were diagnosed 4 months to 14.3 years after irradiation, with a median of 6.1 years, and median age at diagnosis was 10.7 years (range, 5.0–23.1 years). Notably, 11/44 (25%) of tumor-bearing irradiated animals were diagnosed with at least 2 neoplasms.

When grouping the RLEC by lethality dose ranges,[28] incidence of neoplasia was higher in irradiated animals. Tumor-bearing animals comprised 2% of the control population, 11.9% of the <LD10 group, 19.8% of the LD10–50 group, 20% of the LD50–90 group, and 28.6% of the LD90+ group. The log-rank test showed a significantly increased probability for cancer ($P < .0001$) in irradiated monkeys relative to controls (Fig. 2A). Cox regression with adjustment for sex showed a significantly increased hazard over time for cancer occurrence in irradiated monkeys relative to the control group (hazard ratio, 23.06; $P = .002$). Sex was not associated with cancer incidence over time ($P = .12$). Log-rank testing showed a significantly increased probability for sarcoma in the irradiated monkeys relative to nonirradiated controls ($P = .003$), but not carcinoma ($P = .13$).

Among the irradiated animals using age as the time axis with age at irradiation as the entry event, no significant difference was appreciated on log-rank testing (Fig. 2B, $P = .28$) or in Cox regression with adjustment for sex ($P = .41$). Analyses utilizing time since irradiation as the time axis were similar, with nonsignificant results for lethality dose group by log-rank test ($P = .96$) and Cox regression with adjustment for sex and age at irradiation ($P = .99$). While proportions of first neoplasia subtype differed by group in irradiated animals that developed cancer, the differences were not significant (Fig. 2C). However, the incidence of developing more than 1 tumor increased with dose group (<LD10: 0%, LD10–50: 12.5%, LD50–90: 47.1%, LD90+: 25.0%; $P = .04$).

Neoplasms in the RLEC include a high incidence of mesenchymal tumors

Table 2 lists the various tumors diagnosed within the RLEC, and Figure 3 provides representative histopathology and IHC for select tumor types. Mesenchymal neoplasms accounted for 37/61 (61.2%) of total neoplasms in the irradiated group. Sarcomas were the most prevalent neoplasms, accounting for 21/61 (34.4) of the total diagnoses. MNSTs were the most common sarcoma (28.5%). Other common sarcomas in this group included glomus tumors and malignant vascular tumors. Uncommon sarcomas included 1 each of

osteosarcoma, leiomyosarcoma, fibrosarcoma, myxosarcoma, and gastrointestinal stromal tumor. Lymphomas and leukemias were less common, accounting for 5% of total RLEC cancers. Benign mesenchymal tumors accounted for 14/61 (23.0%) of total neoplasms in the RLEC, and the most common diagnoses were leiomyomas and neurofibromas. By contrast, benign mesenchymal tumors represented 16.2% of neoplasia in the Wisconsin aging cohort.[16]

Epithelial neoplasms in the RLEC were less common, accounting for 11/61 neoplasms (18.0%). Hepatocellular and renal cell tumors each represented 27.3% of carcinomas (each 5% of total RLEC cancers). The most common benign epithelial neoplasm in the RLEC was renal adenoma.

Neoplasia was detected in most major organ systems (Fig. 4). The most common anatomic site of neoplasia in the RLEC was the skin and subcutis, with 24 cutaneous/subcutaneous neoplasms (40%). Similar to the population as a whole, most neoplasms in the skin/subcutis were of mesenchymal origin (79.2% of cutaneous/subcutaneous tumors). The most common diagnosis in the skin/subcutis was MNST, representing 16.7% of cutaneous/subcutaneous neoplasia.

MNSTs in the RLEC share transcriptional features with human MNSTs

Human and rhesus MNSTs did not separate in principle components; the top two components accounted for 54.5% of the variance (Fig. 5A). Normalized counts for specific target genes associated with MNST pathogenesis did not show significant differences between human and NHP tumors (adjusted $P > .9$; Fig. 5B). There were 84 differentially expressed genes detected between human and rhesus MNSTs, with P adjusted values <.05. Of these, 63 were upregulated in rhesus MNSTs. The 10 most up-regulated genes were *MYF5*, *KCNC2*, *BPIFB4*, *SLC17A1*, *GJB6*, *MYL7*, *APOA4*, *SLC27A6*, *CNTNAP2*, and *DLK1*, with log-fold changes ranging from 11.7 to 27.6. The 10 most down-regulated genes were *TCHHL1*, *MT4*, *KRT71*, *KRT35*, *LCN9*, *PAGE1*, *PRR9*, *CARTPT*, *XAGE3*, and *SEMG2*. The 5 most upregulated and downregulated genes are labeled in Figure 5C. The most significantly expressed gene by false discovery rate (adjusted $P < .0001$) was RSAD2, with a log-fold increase of 4.4, which is labeled in Figure 5A. The 63 upregulated genes were assessed for gene ontology (GO) enrichment using the online GO Resource. The only enriched pathway detected by GO analysis was hydrogen peroxide metabolic process (GO: 0042743), which showed 38.61-fold enrichment (adjusted P value = .006).

Discussion

This study describes the incidence of neoplasia in a cohort of irradiated rhesus macaques. Similar to previous reports,[13,14] we observed an increased incidence of cancer in irradiated compared to nonirradiated NHP. In our irradiated population, 18% of animals were diagnosed with neoplasia — more than double the 8.2% described by Simmons and Mattison[16] in their report of cancer in aging, nonirradiated macaques. The skin and subcutis were by far the most common sites of neoplasia in the RLEC, although neoplasia was detected in nearly all major organ systems, including hematopoietic, intestinal, hepatobiliary,

cardiovascular, respiratory, skeletal, male and female reproductive, and central nervous systems.

To evaluate the role of irradiation on cancer incidence, log-rank tests and Cox regression analysis were conducted. For these analyses, age as the time axis was selected because cancer is strongly associated with aging, using age from arrival in the RLEC to either diagnosis of the first neoplasm or the monkey's current age or age at death as the time axis and cancer occurrence as the event. In survival models, radiation was strongly associated with increased cancer incidence compared to the controls, but there was no significant difference in cancer incidence between radiation dose groups within irradiated animals. Sex did not have a significant effect on cancer incidence; however, the RLEC population is predominantly male. Interestingly, when examining sarcomas only, there was a significant difference in sarcoma incidence within the irradiated group compared to nonirradiated monkeys; however, there was no significant difference between irradiated and nonirradiated monkeys regarding carcinoma incidence. This is likely due to the low number of carcinomas present in the RLEC. Taken together, these results support that TBI is highly associated with increased neoplasia in monkeys, although dose may not affect cancer incidence.

Irradiated animals in the RLEC exhibited neoplastic phenotypes that differ from what has been reported in nonirradiated monkeys, including cancers uncommon to NHP.[16] Sarcomas and benign mesenchymal tumors comprised the most common neoplastic phenotypes, representing 61% of the tumor population in irradiated monkeys. Sarcomas alone accounted for 38% of all neoplastic diagnoses. By contrast, sarcomas are relatively rare in otherwise clinically healthy, nonirradiated rhesus monkeys; in aging monkeys, sarcomas only account for approximately 4% of neoplastic diagnoses.[16] The most common sarcomas in the RLEC irradiated animals were MNSTs, malignant glomus tumors, and vascular malignancies. These are all relatively rare cancers in rhesus monkeys, and none of these histotypes were observed in aging macaques.[16]

In humans, MNSTs are rare neoplasms, most commonly associated with neurofibromatosis type 1 (NF1), a heritable syndrome that results in loss of heterozygosity in the tumor suppressor gene *NF1*, which is a negative regulator of the RAS signaling pathway.[38] In addition to *NF1*, several studies have indicated that loss of tumor suppression is a common finding in spontaneous MNSTs, including p53, p16, and the PRC2 complex (SUZ12 and EED).[39,40] Other common molecular findings in spontaneous MNSTs include increased expression of the transcription factor YAP1,[41] increased AKT/mTOR pathway activity,[39] and mutations in *ATRX* and *RB1*.[31] MNSTs occur rarely following radiation and comprise about 5% of postradiation sarcomas,[42] which typically occur after radiation therapy for breast cancer and lymphoma.[43] MNSTs are usually positive for the immunohistochemical markers vimentin, S100, and SOX10.[44] In the RLEC, MNSTs represented 10% of all neoplasms (26% of sarcomas) in irradiated NHP and stained positive for S100 and vimentin, similar to humans. In contrast to humans and irradiated NHP in the RLEC, nerve sheath tumors are relatively rare in nonirradiated rhesus monkeys; however, single case reports describe benign nerve sheath tumors.[45] MNSTs were not reported in aging macaques.[16]

RNA sequencing analysis demonstrated similar transcriptional profiles between MNSTs in the RLEC and publicly available RNA data from human MNSTs in the Cancer Genome Atlas sarcoma study. Principle component analysis did not separate MNSTs along species lines, and only 84 genes were significantly differentially expressed between humans and NHP. We also looked specifically at the expression of several genes commonly associated with MNSTs, including *ATRX*, *YAP1*, members of the RAS pathway (*NF1*, *AKT*, *mTOR*), cell cycle regulation (*RB1*, *TP53*), and the PRC2 complex (*SUZ12*, *EED*, *EZH1*, *EZH2*). Directly comparing normalized expression counts between human and RLEC MNSTs for these genes showed no statistically significant differences.

While the gene expression profiles were largely similar, 84 differentially expressed genes were still observed between human and rhesus MNSTs. Of these, 63 genes were upregulated in NHP MNSTs. Gene ontology analysis of these upregulated genes showed enrichment for a single pathway, hydrogen peroxide metabolism, which may be related to oxidative injury. A previous study examining transcriptional differences between spontaneous and radiation therapy-induced sarcomas showed that differential gene expression largely favored pathways associated with oxidative injury in the radiationsarcomas, although peroxide-related metabolic pathways were not specifically observed and MNSTs were not included.[46] Among the highly expressed genes in NHP MNSTs was *GJB6*, a gap junction protein related to *GJB2*. Interestingly, *GJB2* was among the most highly expressed genes in radiation-induced lung injury in a previous study on the RLEC.[25] *RSAD2* demonstrated the most significant differential expression by adjusted *P* value, with a log-fold increase of 4.4. This is a curious finding, as *RSAD2* encodes the viperin protein, an interferon-responsive gene involved in inhibition of viral replication,[47] which may be overexpressed in cancers resistant to oncolytic viruses.[48] Taken together, these findings suggest that there are similar gene expression patterns in human and rhesus monkey MNSTs.

Glomus tumors are rare, usually benign neoplasms in humans that arise from the modified pericytes in the thermoregulatory glomus apparatus in the skin.[49] Malignant and visceral glomus tumors are exceptionally rare in humans, but have been reported.[49–51] Glomus tumors typically stain positive for vimentin, α-SMA, and collagen IV.[52] To our knowledge, glomus tumors have not been described as a consequence of radiation therapy or TBI in humans. In the irradiated monkeys of the RLEC, all of the glomus tumors had malignant histologic features, such as nuclear pleomorphism, visceral locations, tissue invasion, and/or high mitotic rate, and represented 8% of neoplasia (22% of sarcomas). As expected, all RLEC glomus tumors exhibited positive immunohistochemical reactivity for vimentin, α-SMA, and collagen IV. Interestingly, in rhesus macaques, glomus tumors are exceptionally rare, and have only been described in monkeys that received TBI.[14,16,53,54]

Vascular malignancies are rare sarcomas in humans that present with a wide spectrum of histologic features.[55] Hemangioendotheliomas are low-grade malignancies and angiosarcomas/hemangiosarcomas may range from low to high grade.[55] Angiosarcomas are well-described as a severe complication of radiation therapy, particularly after radiation therapy for breast cancer.[56,57] These are typically cutaneous, present years after irradiation, and are uniquely associated with *MYC* amplification.[55–57] Angiosarcomas are classically identified using IHC, whereby the tumors stain positive for the markers vimentin, CD31,

ERG, CD34, factor VIII-related protein, and collagen IV.[55] In the irradiated monkeys of the RLEC, vascular malignancies included angiosarcomas and a single hemangioendothelioma, and comprised 8% of total neoplastic diagnoses (22% of sarcomas). All RLEC vascular malignancies were positive by IHC for vimentin and collagen IV; all but 1 were positive for CD31. In contrast to irradiated RLEC monkeys and humans, vascular malignancies are rare in nonirradiated rhesus monkeys, with sporadic case reports consisting primarily of angiosarcoma/hemangiosarcoma.[58] In the aging study, benign hemangiomas were reported, but no vascular malignancies were described.[16]

Carcinomas were less common in the RLEC irradiated cohort and accounted for 18% of RLEC neoplastic diagnoses in irradiated NHP. Both hepatocellular and renal cell carcinomas were the most common diagnoses, each representing 5% of all RLEC neoplasia (27% of carcinomas). By contrast, carcinomas represent the majority of neoplastic diagnoses in aging, nonirradiated monkeys; the most common cancer in this species is intestinal adenocarcinoma.[16,59,60] Interestingly, intestinal carcinomas have not been detected to date in the RLEC monkeys. Most of the NHP in the RLEC are younger, with the average age of the irradiated animals just under 10 years, and the average age of neoplasia diagnosis is just over 12 years. The average ages at tumor diagnosis of most NHP in the nonirradiated, aging study were over 20 years.[16] This may explain the paucity of intestinal carcinomas, as these young animals that were exposed to radiation developed cancer prior to reaching the age at which intestinal carcinomas are expected to occur.

This cross-sectional study showing the association between TBI and cancer in rhesus monkeys has some limitations. Firstly, the low incidence of cases in the controls and the small number of monkeys in the highest irradiation dose group limited our ability to detect meaningful statistical differences by dose group. Secondly, the population was heterogeneic, with monkeys arriving from different sources, irradiated with a wide range of doses at various ages and with differing lengths of follow-up time by lethality dose group. The RLEC is also predominantly male, limiting the assessment of sex as a factor in radiation-induced cancer. Technical factors such as RNA concentration and integrity, batch effects, and differences in sequencing protocols between the RLEC MNST samples and TCGA samples may have introduced additional variability to the RNA data. This initial description of neoplasia in the RLEC provides a foundation for future studies into mechanisms of radiation-induced cancer.

Conclusions

We describe the incidence of cancer phenotypes within the RLEC of rhesus macaques. Neoplasia in irradiated monkeys of the RLEC had histologic phenotypes distinct from nonirradiated populations.[16] Given the frequency of sarcomas in the irradiated RLEC NHPs relative to the nonirradiated controls and to previous literature, we conclude that total-body ionizing radiation is associated with sarcomagenesis in rhesus macaques. TBI can also explain the wide anatomic distribution of the sarcomas, by inducing malignant transformation of mesenchymal cells, such as nerve sheath cells, fibroblasts, and endothelial cells, which are found in most tissues throughout the body. Future studies will focus on the genetic and additional transcriptional features of these tumors. We anticipate that the

RLEC will elucidate mechanisms that promote sarcoma development in survivors of acute TBI in an animal model that closely recapitulates human biology and radiation-induced disease. Our study indicates the RLEC's potential as an NHP model of cancer as a delayed effect of acute radiation exposure and lays the groundwork for future studies to examine the mechanism of TBI-induced carcinogenesis and sarcomagenesis.

Acknowledgments—

The authors thank the Cline lab technical staff, the Wake Forest Animal Resource Program's clinical support staff, and the support of the Comparative Pathology Laboratory, Cancer Genomics, and Bioinformatics Shared Resources of the Comprehensive Cancer Center of Wake Forest Baptist Medical Center.

This work was supported by National Institutes of Health (NIH)/National Institute of Allergy and Infectious Diseases funding (U01 AI150578, U19 AI67798), NIH training funds (T32 OD010957), a National Cancer Institute Cancer Center Support Grant (P30CA012197) to the Comprehensive Cancer Center of Wake Forest Baptist Medical Center, and an equipment grant from the North Carolina Biotechnology Center (2015-IDG-1006).

References

1. Osaka K, Grant EJ, Kodama K. Japanese legacy cohorts: The life span study atomic bomb survivor cohort and survivors' offspring. J Epidemiol 2018;28:162–169. [PubMed: 29553058]
2. Preston DL, Ron E, Tokuoka S, et al. Solid cancer incidence in atomic bomb survivors: 1958–1998. Radiat Res 2000;168:1–64.
3. Grant EJ, Brenner A, Sugiyama H, et al. Solid cancer incidence among the life span study of atomic bomb survivors: 1958–2009. Radiat Res 2017;187:513–537. [PubMed: 28319463]
4. Osaka K, Cullings HM, Ohishi W, Hida A, Grant EJ. Epidemiological studies of atomic bomb radiation at the Radiation Effects Research Foundation. IJRB 2019;95:879–891. [PubMed: 30676179]
5. Patel SR. Radiation-induced sarcoma. Curr Treat Opt Oncol 2000;1:258–261.
6. Bjerkehagen B, Smastuen MC, Hall KS, et al. Incidence and mortality of second sarcomas — A population-based study. Eur J Cancer 2013;49:3292–3302. [PubMed: 23787025]
7. Menu-Branthomme A, Rubino C, Shamsaldin A, et al. Radiation dose, chemotherapy, and risk of soft tissue sarcoma after solid tumours during childhood. Int J Cancer 2004;110:87–93. [PubMed: 15054872]
8. Schneider U, Sumila M, Robotka J. Site-specific dose-response relationships for cancer induction from the combined Japanese A-bomb and Hodgkin cohorts for doses relevant to radiotherapy. Theor Biol Bed Model 2011;8:27.
9. Rogers J, Gibbs RA. Comparative primate genomics: Emerging patterns of genome content and dynamics. Nat Rev Genet 2014;15:347–359. [PubMed: 24709753]
10. Messaoudi I, Estep R, Robinson B, Wong SW. Nonhuman primate models of human immunology. Antioxid Redox Signal 2011;14:261–273. [PubMed: 20524846]
11. Cline JM, Wood CE. The mammary glands of macaques. Toxicol Pathol 2008;36:134–141.
12. Xia H Progress of non-human primate animal models of cancer. Zoo Res 2011;32:70–80.
13. Kent SP, Pickering JE. Neoplasms in monkeys (Macaca mulatta): Spontaneous and irradiation induced. Cancer 1958;11:138–147. [PubMed: 13500309]
14. Broerse JJ, Bartstra RW, van Bekkum DW, et al. The carcinogenic risk of high dose total body irradiation in non-human primates. Radiother Oncol 2000;54:247–253. [PubMed: 10738083]
15. Wood DH. Long-term mortality and cancer risk in irradiated rhesus monkeys. Radiat Res 1991;126:132–140. [PubMed: 1850849]
16. Simmons HA, Mattison JA. The incidence of spontaneous neoplasia in two populations of captive rhesus macaques (Macaca mulatta). Antioxid Redox Signal 2011;14:221–227. [PubMed: 20524847]

17. Kent SP. Spontaneous and induced malignant neoplasms in monkeys. Ann NY Acad Sci 1960;85:819–827. [PubMed: 13752561]
18. Farese AM, Cohen MV, Katz BP, et al. A nonhuman primate model of the hematopoietic acute radiation syndrome plus medical management. Health Phys 2012;103:367–382. [PubMed: 22929469]
19. Carrier CA, Elliot TB, Ledney GD. Real-time telemetric monitoring in whole-body 60Co gamma-photon irradiated rhesus macaques (Macaca mulatta). J Med Primatol 2010;1–9. [PubMed: 19811605]
20. Kavanagh K, Dendinger MD, Davis AT, et al. Type 2 diabetes is a delayed late effect of whole-body irradiation in nonhuman primates. Radiat Res 2015;183:398–406. [PubMed: 25811716]
21. Bacarella N, Ruggiero A, Davis AT, et al. Whole body irradiation induces diabetes and adipose insulin resistance in nonhuman primates. Int J Radiat Oncol Biol Phys 2020;106:878–886. [PubMed: 31805366]
22. Hanbury DB, Peiffer AM, Dugan G, et al. Long-term cognitive functioning in single-dose total-body gamma-irradiated rhesus monkeys (Macaca mulatta). Radiat Res 2016;186:447–454. [PubMed: 27740889]
23. Andrews RN, Metheny-Barlow LJ, Peiffer AM, et al. Cerebrovascular remodeling and neuroinflammation is a late effect of radiation-induced brain injury in non-human primates. Radiat Res 2017;187: 599–611. [PubMed: 28398880]
24. Andrews RN, Bloomer EG, Olson JD, et al. Non-human primates receiving high-dose total-body irradiation are at risk of developing cerebrovascular injury years postirradiation. Radiat Res 2020;194:277–287. [PubMed: 32942304]
25. Thakur P, DeBo R, Dugan GO, et al. Clinicopathologic and transcriptomic analysis of radiation-induced lung injury in nonhuman primates. Int J Radiat Oncol Biol Phys 2021;111:249–259. [PubMed: 33848608]
26. DeBo RJ, Lees CJ, Dugan GO, et al. Late effects of total-body gamma irradiation on cardiac structure and function in male rhesus macaques. Radiat Res 2016;186:55–64. [PubMed: 27333082]
27. Hale LP, Rajam G, Carlone GM, et al. Late effects of total body irradiation on hematopoietic recovery and immune function in rhesus macaques. PLoS ONE 2019;14:e0210663. [PubMed: 30759098]
28. MacVittie TJ, Farese AM, Jackson W. The hematopoietic syndrome of the acute radiation syndrome in rhesus macaques: A systematic review of the lethal dose response relationship. Health Phys 2015;109:342–366. [PubMed: 26425897]
29. Yu JZ, Lindeblad M, Lyubimov A, et al. Subject-based versus population-based care after radiation exposure. Radiat Res 2015;184:46–55. [PubMed: 26121229]
30. Leary S, Underwood W, Anthony R, et al. AVMA Guidelines for the Euthanasia of Animals: 2020 Edition. American Veterinary Medical Association, Schaumburg, IL 2020.
31. Abeshouse A, Adebamowo C, Adebamowo SN, et al. Comprehensive and integrated genomic characterization of adult soft tissue sarcomas. Cell 2017;171:950–965. [PubMed: 29100075]
32. Dobin A, Davis CA, Schlesinger F, et al. STAR: Ultrafast universal RNA-seq aligner. Bioinformatics 2013;29:15–21. [PubMed: 23104886]
33. Liao Y, Smyth GK, Shi W. featureCounts: An efficient general purpose program for assigning sequence reads to genomic features. Bioinformatics 2014;30:923–930. [PubMed: 24227677]
34. Gu Y-H, Cui X-W, Ren J-Y, et al. Selection of internal references for RT-qPCR assays in neurofibromatosis type 1 (NF1) related Schwann cell lines. PLoS ONE 2021;16 e0241821. [PubMed: 33630851]
35. Risso D, Ngai J, Speed TP, Dudoit S. Normalization of RNA-seq data using factor analysis of control genes or samples. Nat Biotechnol 2014;32:896–902. [PubMed: 25150836]
36. Thomas PD, Campbell MJ, Kejariwal A, et al. PANTHER: A library of protein families and subfamilies indexed by function. Genome Res 2003;13:2129–2141. [PubMed: 12952881]
37. Mesalu T, Vilo J. ClustVis: A web tool for visualizing clustering of multivariate data using principal component analysis and heatmap. Nucleic Acids Res 2015;43:W566–W570. [PubMed: 25969447]

38. Yap Y-S, McPherson JR, Ong C-K, et al. The NF1 gene revisited – from bench to bedside. Oncotarget 2014;5:5873–5892. [PubMed: 25026295]
39. Lemberg KM, Wang J, Pratilas CA. From genes to -omics: The evolving molecular landscape of malignant peripheral nerve sheath tumor. Genes 2020;11:691.
40. Lee W, Teckie S, Wiesner T, et al. PRC2 is recurrently inactivated through EED or SUZ12 loss in malignant peripheral nerve sheath tumors. Nat Genet 2014;46:1227–1232. [PubMed: 25240281]
41. Isfort I, Elges S, Cyra M, et al. Prevalence of the hippo effectors YAP1/ TAZ in tumors of soft tissue and bone. Nat Sci Rep 2019;9:19704.
42. LaFemina J, Qin L-X, Moraco NH, et al. Oncologic outcomes of sporadic, neurofibromatosis-associated, and radiation-induced malignant peripheral nerve sheath tumors. Ann Surg Oncol 2013;20:66–72. [PubMed: 22878618]
43. Yamanaka R, Hayano A. Radiation-induced malignant peripheral nerve sheath tumors: A systematic review. World Neurosurg 2017;105:961–970. [PubMed: 28602926]
44. Nielsen GP, Chi P. Malignant peripheral nerve sheath tumour. WHO Editorial Board, eds. The WHO Classification of Tumours: Soft Tissue and Bone Tumours. 5th ed. Lyon, France: International Agency for Research on Cancer; 2020:254–257.
45. Alves DA, Bell TM, Benton C, et al. Giant thoracic schwannoma in a rhesus macaque (*Macaca mulatta*). JAALAS 2010;49:868–872. [PubMed: 21205456]
46. Hadj-Hamou N-S, Ugolin N, Ory C, et al. A transcriptome signature distinguished sporadic from postradiotherapy radiation-induced sarcomas. Carcinogenesis 2011;32:929–934. [PubMed: 21470956]
47. Mattijssen S, Prujin GJ. Viperin, a key player in the antiviral response. Microbe Infect 2012;14:419–426.
48. Goradel NH, Alizadeh A, Hasseinzadeh S, et al. Oncolytic virotherapy as promising immunotherapy against cancer: mechanisms of resistance to oncolytic viruses. Future Oncol 2022;18:245–259. [PubMed: 34821517]
49. Wood TR, McHugh JB, Siegel GW. Glomus tumors with malignant features of the extremities: A case series. Clin Sarcoma Res 2020;10:20. [PubMed: 33133513]
50. Jang S-H, Cho HD, Lee J-H, et al. Mediastinal glomus tumor: A case report and literature review. J Pathol Transl Med 2015;49:520–524. [PubMed: 26265686]
51. Lambda G, Rafiyath SM, Kaur H, et al. Malignant glomus tumor of kidney: The first reported case and review of literature. Hum Pathol 2011;42:1200–1205. [PubMed: 21333326]
52. Specht K, Antonescu CR. Glomus tumour. WHO Editorial Board, eds.. The WHO Classification of Tumours: Soft Tissue and Bone Tumours. 5th ed. Lyon, France: International Agency for Research on Cancer; 2020:179–181.
53. Hubbard GB, Fanton JW, Harvey RC, Wood DH. Paralysis due to a glomangioma in a *Macaca mulatta*. Lab Anim Sci 1984;34:614–615. [PubMed: 6097764]
54. Hubbard GB, Wood DH. Glomangiomas in four irradiated Macaca mulatta. Vet Pathol 1984;21:609–610. [PubMed: 6097012]
55. Thway K, Billings SD. Angiosarcoma. WHO Editorial Board, eds.. The WHO Classification of Tumours: Soft Tissue and Bone Tumours. 5th ed. Lyon, France: International Agency for Research on Cancer; 2020:176–178.
56. Lucas DR. Angiosarcoma, radiation-associated angiosarcoma, and atypical vascular lesion. Arch Pathol Lab Med 2009;133:1804–1809. [PubMed: 19886715]
57. Thibodeau BJ, Lavergne V, Dekhne N, et al. Mutational landscape of radiation-associated angiosarcoma of the breast. Oncotarget 2018;9:10042–10053. [PubMed: 29515789]
58. Beck AP, Gray SB, Chaffee BK. Disseminated hemangiosarcoma in a juvenile rhesus macaque (Macaca mulatta). Comp Med 2016;66:246–253. [PubMed: 27298251]
59. Dray BK, Raveendran M, Harris RA, et al. Mismatch repair gene mutations lead to lynch syndrome colorectal cancer in rhesus macaques. Genes Cancer 2018;9:142–152. [PubMed: 30108684]

60. Harbison CE, Taheri F, Knight H, Miller AD. Immunohistochemical characterization of large intestinal adenocarcinoma in the rhesus macaque (Macaca mulatta). Vet Pathol 2015;52:732–740. [PubMed: 25367367]

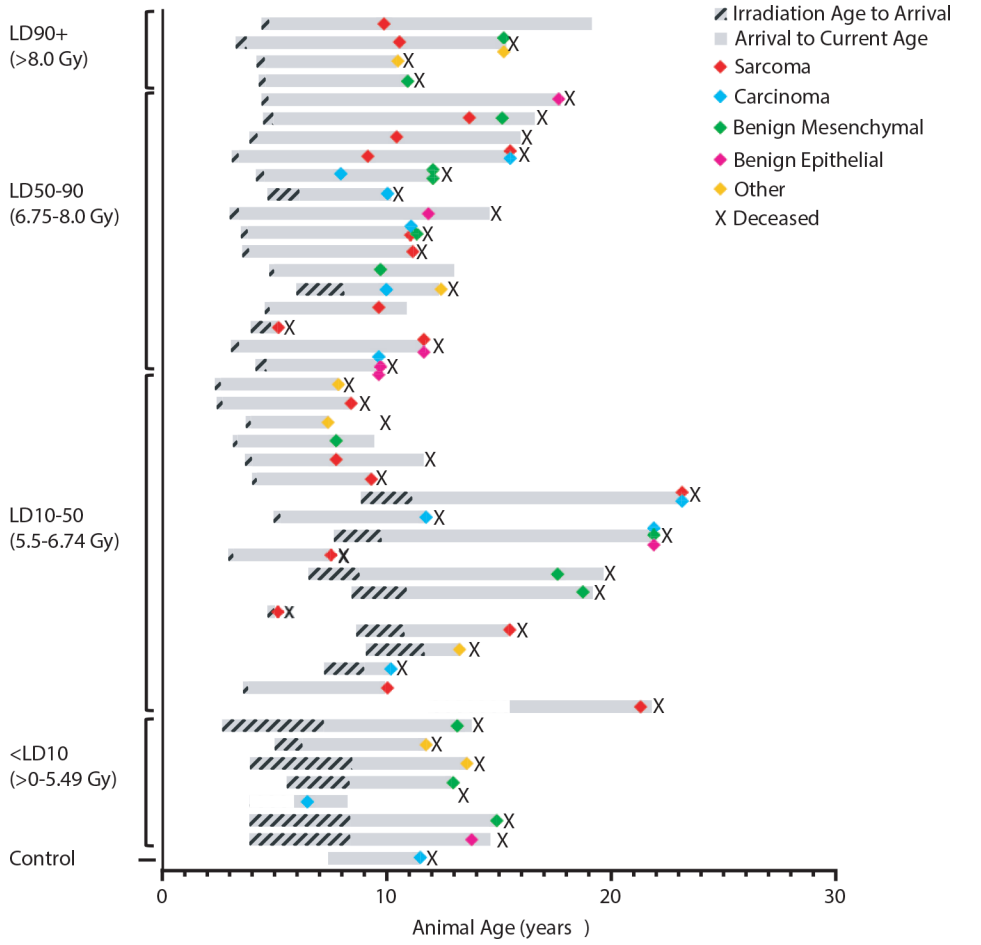

Fig. 1.

Occurrence of neoplasia in long-term nonhuman primate survivors of total-body irradiation. Each bar represents a single animal, plotted on its own life span. Animals are listed in descending order of radiation dose, grouped by lethality dose (LD) range. Bars begin at the age of irradiation and end at the animal's current age or age of death (deceased animals indicated by **X**). Colored icons indicate the age of diagnosis for each tumor described for each animal. Colors indicate tumor type (see key). Hashed grey regions indicate the period of life between irradiation and arrival at Wake Forest School of Medicine (WFSM). Solid grey regions indicate the period of observation within the radiation late effects cohort.

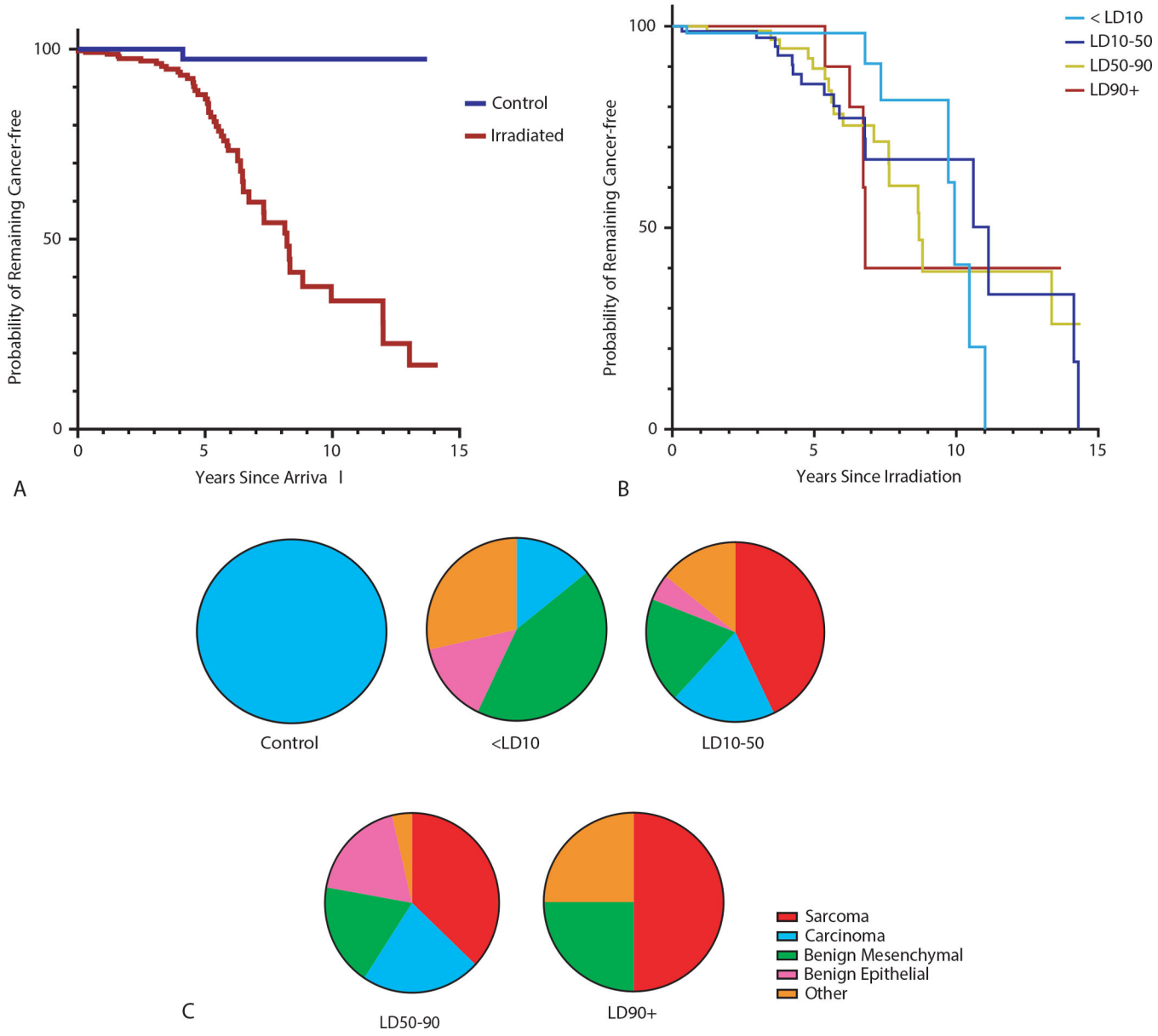

Fig. 2.

Radiation and neoplasia incidence. (A) Kaplan-Meier plot showing probability of remaining tumor-free in irradiated monkeys compared to nonirradiated controls. The time interval (x-axis) is set from the age at arrival to the age at neoplasia diagnosis or current age. There is a marked difference between the groups, with irradiated animals less likely to remain tumor-free with time (log rank test $P < .0001$). (B) Kaplan-Meier plot demonstrating probability of remaining cancer free in each radiation lethality dose (LD) group. There is no significant difference between dose groups (log rank test $P = .28$). The time interval (x-axis) is set from the age at irradiation to the age at diagnosis. (C) Proportions of earliest-diagnosed neoplasm types within each lethality dose group.

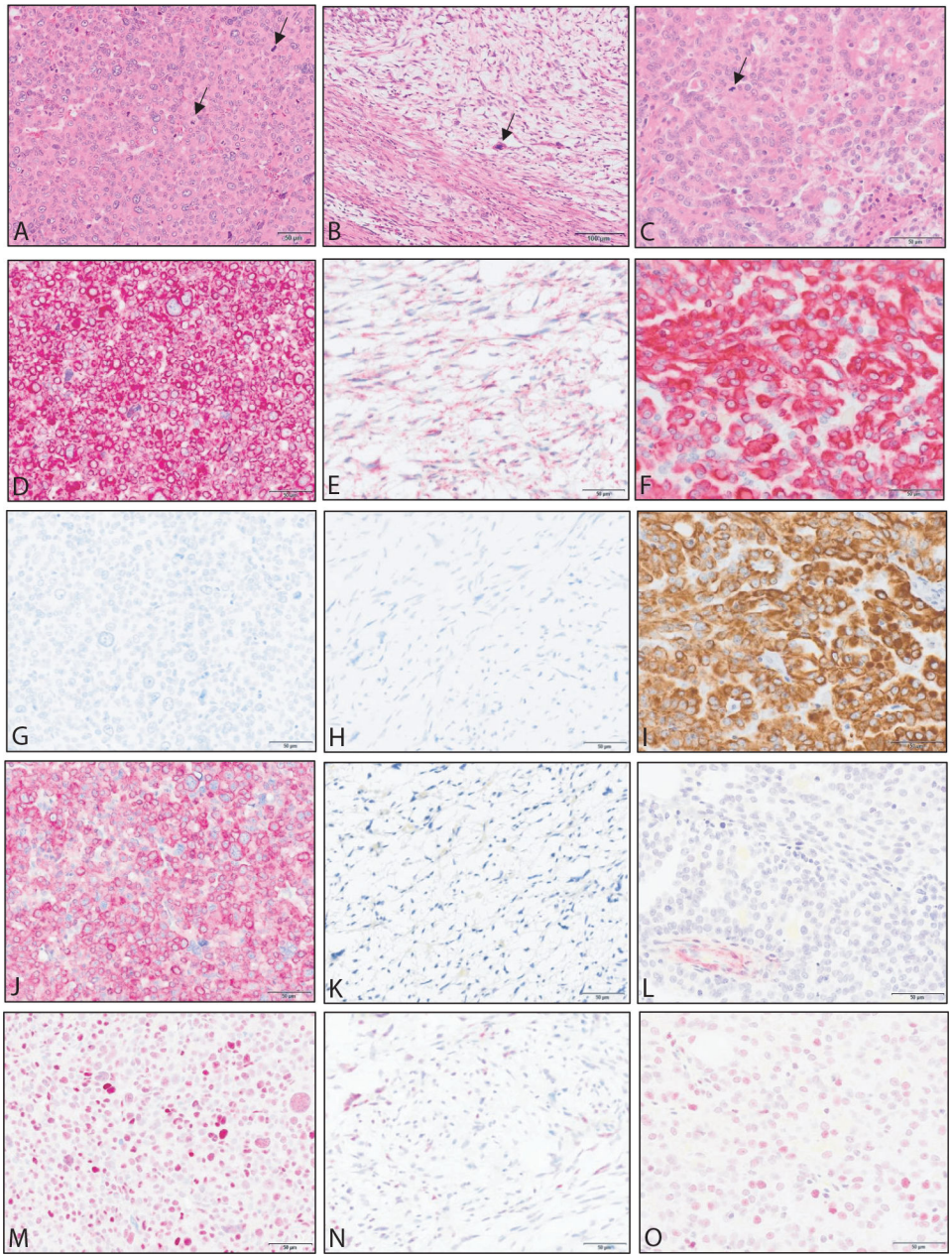

Fig. 3.

Examples of neoplasia observed in the radiation late effects cohort. Images in the left column are from a renal glomus tumor. Images in the middle column are from a cutaneous malignant nerve sheath tumor. Images in the right column are from a renal cell carcinoma. Stains include hematoxylin and eosin (A-C) and immunohistochemistry for vimentin (D-F), pancytokeratin (G-I), α-smooth muscle actin (J-L), and p53 (M-O). Arrows in hematoxylin and eosin sections indicate mitotic figures.

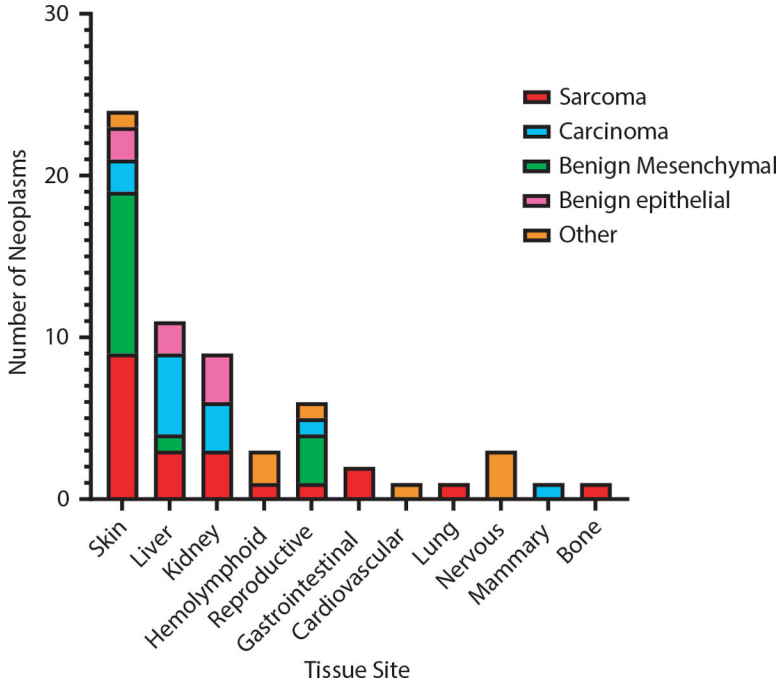

Fig. 4.

Tissue site incidence of neoplasia in nonhuman primate Radiation Late Effects Cohort (RLEC). The majority of neoplasms are of mesenchymal origin (benign and malignant), and the highest incidence of neoplasia is in the skin/subcutis. There is also a notable incidence of hepatic and renal epithelial neoplasia.

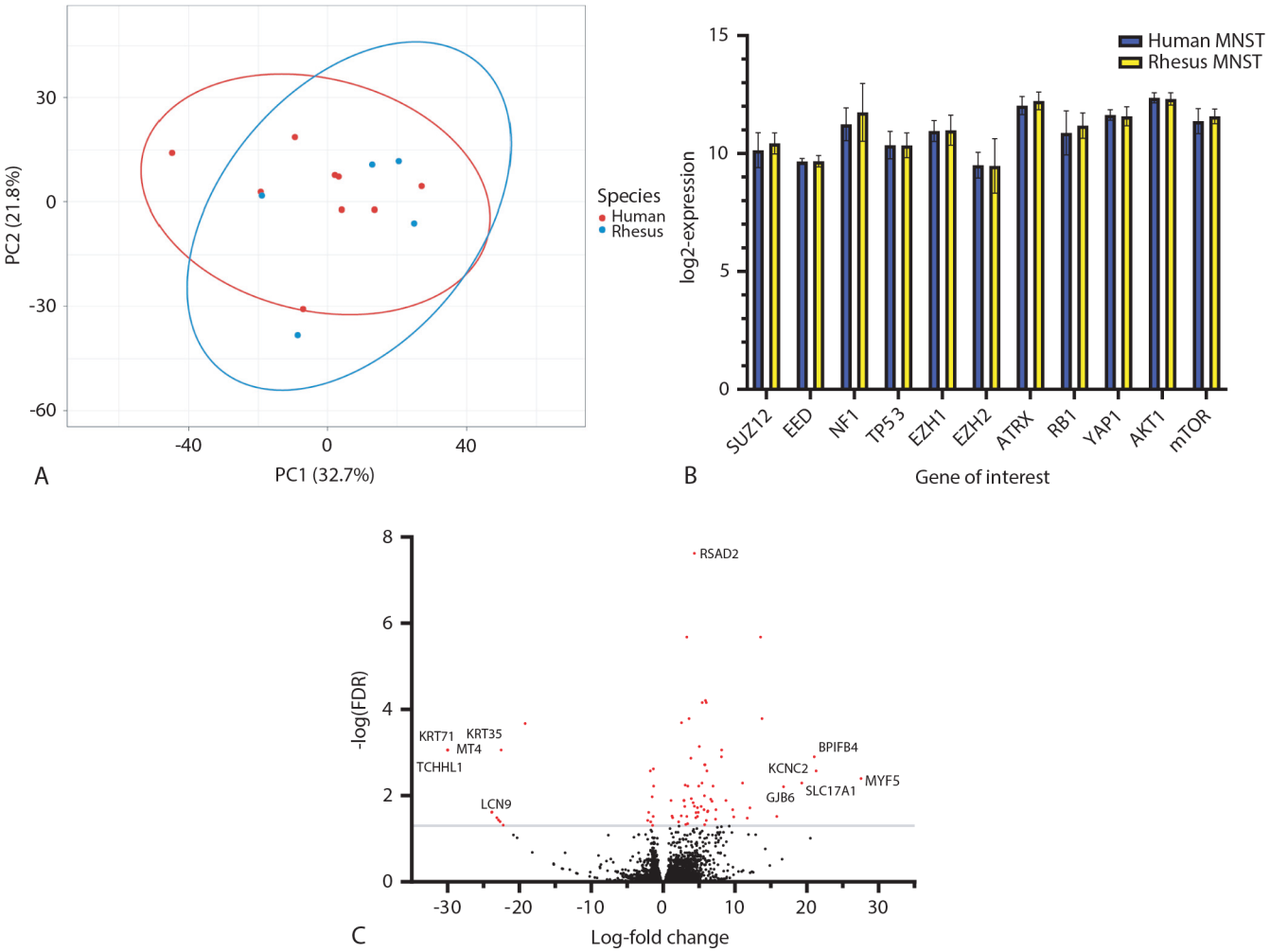

Fig. 5.

Differential gene expression between human and radiation late effects cohort (RLEC) rhesus malignant nerve sheath tumors (MNSTs). (A) Principle component analysis of top 1200 most variably expressed genes between all human and rhesus MNST samples. Samples do not separate by species or form distinct groups along either PC1 or PC2. Ellipses represent 95% confidence intervals. (B) Log-transformed expression values for 11 select MNST-relevant genes. There are no statistically significant differences between human and rhesus MNSTs in any of these genes, after correcting for multiple comparisons (adjusted $P > .9$). (C) Volcano plot of differential expression of 12,826 genes. Log-fold change is represented on the x-axis, and the -log of the false discovery rate (FDR) is on the y-axis. Genes were considered significantly differentially expressed if -log (FDR) > 1.3 (gray line) and are highlighted in red (n = 86). Gene symbols indicate the most up-regulated (*MYF5*, *KCNC2*, *BPIFB4*, and *GJB6*) and most down-regulated (*TCHHL1*, *MT4*, *KRT71*, *KRT35*, *LCN9*) genes by log-fold change. Note that the points for the *TCHLL1*, *MT4*, *KRT71*, and *KRT35* all tightly overlap in the figure at −30 log-fold change.

Table 1

Population demographic information of nonhuman primate radiation late effects cohort

Dose group (Gy) (MacVittie et al[28])	Dose range (Gy)median (min-max range)	Number of animals (% male)	Current age (y) median (min-max range)	Age at irradiation (y) median (min-max range)	Age at arrival (y) median (min-max range)	Median follow-up time since arrival (y)	Number of animals with cancer	Number of cancers	Age at first cancer observation (y) median (min-max range)
Control (0)	0	51 (92)	15.6 (6.8–23.2)	NA	7.0 (2.4–20.0)	6.0	1	1	11.5
<LD10 (0.01–5.49)	4.0 (1.14–5.0)	59 (62)	7.5 (5.1–14.9)	5.0 (2.7–8.2)	4.9 (2.6–10.3)	3.9	7	7	11.8 (6.4–14.9)
LD10-50 (5.5–6.74)	6.5 (5.5–6.73)	79 (77)	5.0–23.1 (10.1)	4.6 (2.3–15.5)	5.2 (2.6–16.0)	3.9	16	19	11.0 (5.0–23.1)
LD50-90 (6.75–7.99)	6.8 (6.75–7.85)	87 (66)	2.7–19.2 (7.9)	3.9 (2.3–7.0)	4.9 (2.6–9.9)	3.3	17	29	9.7 (5.2–17.8)
LD90+ (>8.0)	8.1 (8–8.5)	14 (93)	3.8–19.2 (10.3)	3.7 (3.2–5.1)	4.2 (3.5–5.5)	6.2	4	6	10.2 (9.8–11.0)

Abbreviation: LD = lethality dose.

Table 2

Summary of neoplastic diagnoses in nonhuman primate radiation late effects cohort

Diagnosis	Number observed (irradiated)	Number observed (controls)	Anatomic sites
Sarcoma			
MNST	6	0	Skin/subcutis, liver, kidney
Malignant glomus tumor	5	0	Skin/subcutis, kidney, seminal vesicles, liver
Endothelial malignancies	5	0	Skin/subcutis, spleen, liver, lung
Fibrosarcoma	1	0	Skin/subcutis
Leiomyosarcoma	1	0	Small intestine
Myxosarcoma	1	0	Skin/subcutis
Osteosarcoma	1	0	Skull
GIST	1	0	Colon
Carcinoma			
HCC	3	1	Liver
RCC	3	0	Kidney
Biliary carcinoma	1	0	Liver
Mammary carcinoma	1	0	Mammary gland
BCC	1	0	Skin/subcutis
SCC	1	0	Skin/subcutis
Trophoblastic tumor	1	0	Uterus
Benign mesenchymal			
Leiomyoma	4	0	Uterus, liver
Neurofibroma	3	0	Skin/subcutis
Lipoma	3	0	Skin/subcutis
Fibroma	2	0	Skin/subcutis
Chondrolipoma	1	0	Skin/subcutis
Hemangioma	1	0	Skin/subcutis
Benign epithelial/adenoma			
Renal adenoma	3	0	Kidney
Benign follicular tumor	2	0	Skin/subcutis
Hepatocellular adenoma	1	0	Liver

Diagnosis	Number observed (irradiated)	Number observed (controls)	Anatomic sites
Biliary adenoma	1	0	Liver
Other			
Glioblastoma	1	0	Brain
Melanocytoma	1	0	Skin/subcutis
Meningioma	1	0	Brain
Lymphoma	2	0	Brain, mediastinum
AML	1	0	Bone marrow
Leydig cell tumor	1	0	Testis
Chemoreceptor tumor	1	0	Heart base

Abbreviations: AML = acute myeloid leukemia; BCC = basal cell carcinoma; GIST = gastrointestinal stromal tumor; HCC = hepatocellular carcinoma; MNST = malignant nerve sheath tumor; NHP = nonhuman primate; RCC = renal cell carcinoma; RLEC = radiation late effects cohort; SCC = squamous cell carcinoma.